Thus, the observation and identification of the trapped-ion instability has been seen in many ways. These are as follows: the dependence of the wave amplitude on collisionality was in the range and in the manner predicted for the trapped-ion instability; the instability existed only on the density gradient and it existed only when and where there were trapped particles; and the observed frequency of the trapped-ion instability was at the predicted frequency ($\frac{1}{2}\delta\omega_e$*) and showed the proper dependence on trapped fraction. Although other experiments have operated in the proper collisionality range for the trapped-ion instability[10,11] they were unable to satisfy requirement (1), $\omega_r \ll \omega_{bi}$. This experiment satisfied all of the requirements and provides the first positive identification of the dissipative trapped-ion instability.

This research was supported by the National Science Foundation under Grant No. ECS79-17033 and by the Research Corporation.

[1]B. B. Kadomtsev and O. P. Pogutse, Zh. Eksp. Teor. Fiz. 51, 1734 (1966) [Sov. Phys. JETP 24, 1172 (1967)].

[2]M. N. Rosenbluth, D. W. Ross, and D. P. Kostomarov, Nucl. Fusion 12, 3 (1972).

[3]H. Eubank *et al.*, in *Proceedings of the Seventh International Conference on Plasma Physics and Controlled Nuclear Fusion Research, Innsbruck, Austria, 1978* (International Atomic Energy Agency, Vienna, Austria, 1979), p. 167.

[4]R. Marchand, W. M. Tang, and G. Rewoldt, Phys. Fluids 23, 1164 (1980).

[5]G. A. Navratil, J. Slough, and A. K. Sen, to be published.

[6]S. C. Prager, T. C. Marshall, and A. K. Sen, Plasma Phys. 17, 785 (1975).

[7]D. P. Dixon, A. K. Sen, and T. C. Marshall, Plasma Phys. 20, 225 (1977).

[8]D. Brossier, P. Deschamps, and C. Renard, Phys. Rev. Lett. 26, 124 (1971).

[9]D. P. Grubb and G. A. Emmert, Phys. Fluids 22, 770 (1979).

[10]M. Okabayashi and R. Freeman, Phys. Fluids 15, 359 (1972).

[11]J. R. Drake, Phys. Fluids 20, 1013 (1977).

Helical and Nonhelical Turbulent Dynamos

M. Meneguzzi
Centre National de la Recherche Scientifique and Section d'Astrophysique, Division de la Physique, Centre d'Etudes Nucléaires de Saclay, F-91191 Gif-Sur-Yvette, France

and

U. Frisch
Centre National de la Recherche Scientifique, Observatoire de Nice, F-06007 Nice, France

and

A. Pouquet[a]
Centre National de la Recherche Scientifique, Observatoire de Meudon, F-92190 Meudon, France

(Received 13 April 1981)

Direct numerical simulations of three-dimensional magnetohydrodynamic turbulence with kinetic and magnetic Reynolds numbers up to 100 are presented. Spatially intermittent magnetic fields are observed in a flow with nonhelical driving. Small-scale helical driving produces strong large-scale nearly force-free magnetic fields.

PACS numbers: 51.60.+a, 47.65.+a, 52.30.+r

The stretching of magnetic field lines by turbulent motions in a conducting fluid is one of the most frequently invoked mechanisms for the generation of the magnetic fields of the earth, the sun, stars, and galaxies.[1] It may also lead to undesirable magnetic fields in the liquid sodium cooling system of large breeder reactors.[2,3] When the magnetic Reynolds number R^M exceeds a critical value R_c^M, the stretching is sufficiently strong to overcome the diffusive effect of Joule dissipation, thereby leading to dynamo action. Specifically, consider a statistically stationary turbulent flow with no magnetic field. Let a weak seed magnetic field be introduced. For $R^M < R_c^M$, the same stationary state is recovered asymptotically in time. For $R^M > R_c^M$, the flow bifurcates to a new statistically stationary state. In this nonlinear dynamo regime, the Lorentz force, by

its reaction on the flow, prevents indefinite growth of the magnetic field. This problem cannot be studied within the kinematic[4,5] framework (prescribed velocity); it requires the complete magnetohydrodynamic (MHD) equations:

$$(\partial_t - \nu\nabla^2)\vec{v} = -(\vec{v}\cdot\nabla)\vec{v} + (\vec{b}\cdot\nabla)\vec{b} - \nabla p + \vec{f},$$

$$(\partial_t - \eta\nabla^2)\vec{b} = -(\vec{v}\cdot\nabla)\vec{b} + (\vec{b}\cdot\nabla)\vec{v},$$

$$\nabla\cdot\vec{v} = \nabla\cdot\vec{b} = 0.$$

Here $\vec{v}$ is the velocity, $\vec{b}$ the magnetic field (rescaled to give it dimensions of a velocity), p is the total pressure (kinetic and magnetic), ν and η are the viscosity and magnetic diffusivity, and $\vec{f}$ is a force which drives the flow. Incompressibility is assumed.

The first numerical simulation of three-dimensional MHD turbulence was performed by Pouquet and Patterson[6]; in this decay calculation, at best temporary magnetic field enhancement is observed. A genuine nonlinear dynamo effect was obtained recently by Gilman and Miller.[7] Theirs is a convectively driven dynamo in a spherical shell, a configuration used to model some aspects of the solar dynamo.

The turbulent dynamo in the nonlinear regime can also be explored by using statistical closure techniques. For nonhelical turbulence, Léorat, Pouquet, and Frisch[3] obtain R_c^M's of the order of a few tens. In the helical case, where the flow is not statistically mirror symmetric, they find that R_c^M can be substantially decreased. This is particularly noticeable when there is a clear separation between energy-containing scales and the largest scale of the flow, so that small-scale helicity can destabilize large-scale magnetic fields by the α effect.[5]

Investigating such questions by direct numerical simulation requires a very high resolution in order to attain sufficiently high R^M's and/or to achieve sufficient scale separation. It then seems advisable, at least for a first attempt, to minimize geometric constraints. We assume here 2π periodicity in all three space directions. The flow is driven by random forces. We use Gaussian statistics, δ correlated in time, homogeneous and isotropic, with prescribed energy and helicity injection spectra F_k^V and $\tilde{F}_k^V$. Kinetic and magnetic Reynolds numbers are defined by

$$R^V = l_0 v_0/\nu \text{ and } R^M = l_0 v_0/\eta$$

in terms of the integral scale l_0 and the rms velocity v_0.

The numerical integration of the MHD equations is done by a pseudospectral method.[8] Two codes were developed for the National Center for Atmosperic Research CRAY-1 computer, a 32^3 (in core) which takes 0.5 s per time step and 64^3 (out of core) which takes 16 s per time step (mostly input/output). For unit Prandtl number ν/η, the maximum Reynolds numbers which can be reached without substantial truncation errors are about 40 and 100, respectively.

Nonhelical dynamo: Intermittency.—In nonhelical flows, there is no α effect and the small-scale motion produces essentially a turbulent diffusion of the magnetic field. As noted by Kraichnan and Nagarajan,[9] this may possibly suppress dynamo action.[10] Imposing zero mean helicity in a numerical simulation will nevertheless produce rather strong temporal fluctuations of the total (space integrated) helicity. This can be overcome by choosing a random force which is antisymmetric under space reversal on each realization. The resulting velocity field is also antisymmetric and, hence, has zero total helicity.[11] The energy injection spectrum chosen for the simulation is of the form $F_k^V \sim k^4 \exp(-k^2)$, which has most of the injection taking place near the minimum wave number ($k_{\min}=1$) and, hence, allows the highest possible R^M's (about 100 with the 64^3 code). The mean kinetic energy injection rate ϵ^V (integral of F_k^V) is taken equal to 1. The Prandtl number is 1, with $\nu = 1.2\times10^{-2}$, the lowest realizable value. There is a starting phase, with no magnetic field, during which the Navier-Stokes equation is integrated to a statistical steady state. This requires a few eddy-turnover times (approximately one in this calculation). At time t_1, the beginning of the dynamo phase, a weak magnetic seed is introduced, with $E^M(t_1)/E^V(t_1) = 0.02$. Here, E^V and E^M are the kinetic and magnetic energies per unit mass. The MHD equations are then integrated for more than 10 turnover times. The evolution of E^V and E^M is shown in Fig. 1. The ratio E^M/E^V grows to about 0.1 in 2 turnover times. After that, there appears to be a statistical steady state with only gentle fluctuations in E^M. The Reynolds numbers ($R^V = R^M$) are then about 100. Direct numerical simulation thus supports the prediction of closure calculations[3] concerning the existence of nonhelical dynamos. Further evidence will be given later in this section. The reason why E^V has strong fluctuations in both the starting and the dynamo phases (cf. Fig. 1) is twofold: There are only a few Fourier modes in the energy-carrying region, and they are being kicked independently at each time step.[12]

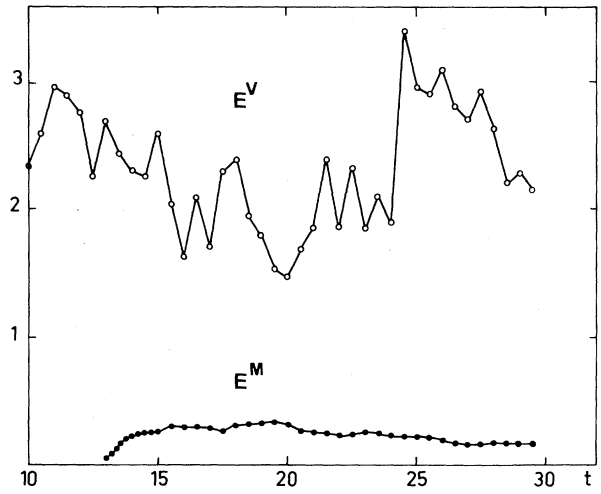

FIG. 1. Turbulent dynamo with nonhelical driving. Temporal variation of kinetic (E^V) and magnetic (E^M) energy. Reynolds numbers are $R^V = R^M \approx 100$. The time unit is the eddy-turnover time l_0/v_0.

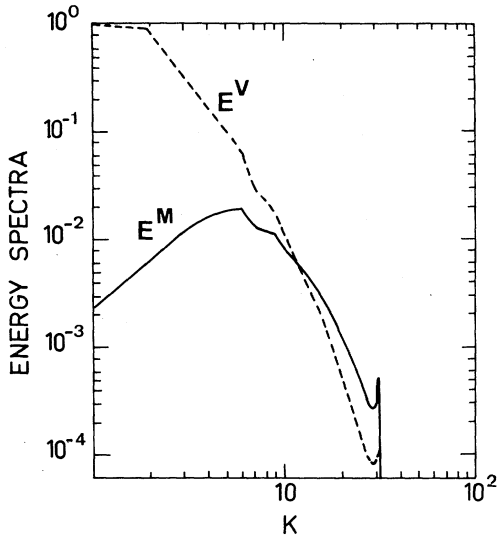

FIG. 2. Kinetic (E^V) and magnetic (E^M) energy spectra at $t = 27$. Nonhelical dynamo with $R^V = R^M \approx 100$.

The dynamo phase has a number of interesting features. In Fig. 2, we show the kinetic and magnetic energy spectra E_k^V and E_k^M at $t = 27$. Note that there is a slight excess of magnetic energy at high wave numbers, as previously found in closure calculations.[3,13] The most striking feature is found in physical space. At time $t = 27$, the supremum over space of b is ≈ 3, comparable to the supremum of v which is ≈ 5. Recall that there is only 10% magnetic energy. This suggests that $\vec{b}$ is intermittent, i.e., concentrated in small regions of physical space. This is indeed seen in Fig. 3, where we give, at $t = 23$, a three-dimensional perspective of the regions where b is within less than 5% of its maximum. A similar cloud picture for v shows essentially one solid cube with a few indentations. No particularly obvious correlation has been found between the intermittent high-b regions and the intermittent high-vorticity regions also observed in nonmagnetic turbulence.[14] The intermittent magnetic structures can be followed in time; they have a lifetime of about one eddy-turnover time. We believe that our simulation, which has only 10% magnetic energy, is just slightly supercritical.[15] It is possible that we are just faced with transitional intermittency. Note that purely temporal intermittency has been observed in systems with a few degrees of freedom which undergo a bifurcation from a turbulent regime to another one with more degrees of freedom excited.[16]

The 64^3 run has taken over 20 h on the CRAY-1 computer. This is not practical for exploring the parameter space, e.g., varying R^M. In the 32^3 simulations, at unit Prandtl number, the highest reliable R^M is about 40 and gives only temporary enhancement of $\vec{b}$. At Prandtl numbers of about

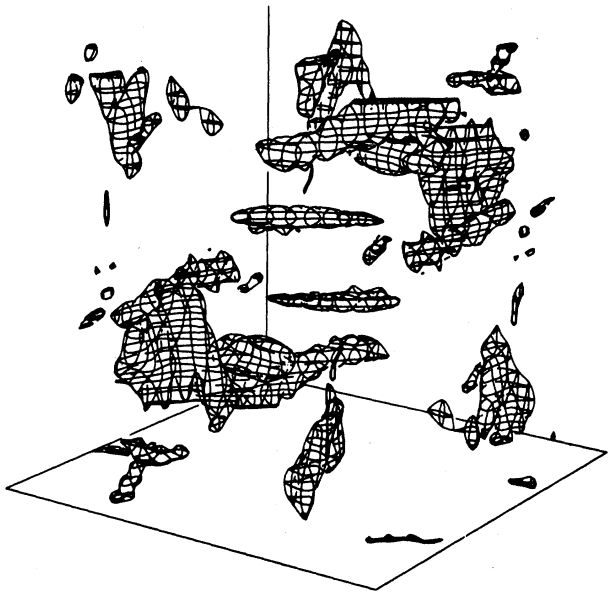

FIG. 3. Spatial intermittency of magnetic field $\vec{b}$ in the nonhelical dynamo at $t = 23$, with $R^V = R^M \approx 100$. The shaded regions have b within less than 5% of its maximum value.

3, higher R^M's (up to about 65) become accessible and a dynamo effect is recovered. By substantially decreasing the R^V (to about 20), it is likely that we provide enough small-scale dissipation to prevent truncation errors. This procedure was also used by Gilman and Miller.[7] We used this procedure here to explore the critical region. For the three values 35, 45, and 65 of R^M, we found steady-state ratios E^M/E^V, respectively, of 0, 0.11, and 0.25. Here E^V and E^M are time-averaged values. For $R^M=45$, which is probably just supercritical, E^M has very strong temporal fluctuations. For $R^M=65$, the temporal fluctuations are somewhat milder; this run was continued for more than one Joule decay time of the energy-carrying eddies, thereby providing somewhat stronger support for the existence of a nonhelical dynamo than given by the $R^V=R^M=100$ run. Spatial intermittency of $\vec{b}$ (slightly stronger than in the $R^M=100$ run) is also observed.

Helical dynamo: Buildup of large-scale magnetic fields.—To favor helicity effects, the ratio of the integral scale l_0 to the spatial period 2π must be small. A drawback is that we severely decrease the maximum Reynolds number which can be simulated with a given resolution. This can be overcome by a modification of the dissipative terms. In Fourier space, instead of νk^2 and ηk^2, we use $\nu' k^{2\delta}$ and $\eta' k^{2\delta}$ with a "dissipativity" $\delta > 1$. This allows us to keep reasonably high Reynolds numbers, in spite of the decrease in l_0. It may be shown that the large-scale dynamics remain essentially unaffected as long as δ is small compared to the spectral resolution (ratio of maximum to minimum wave number).

Our helical simulation is characterized by the following parameters. The injection spectrum is $\sim k^4 \exp(-0.08k^2)$, which peaks at $k=5$. The mean injection rate is $\epsilon^V=2$. Helicity injection is maximal ($\tilde{F}_k{}^V = kF_k{}^V$). The resulting turnover time at injection is $t_0 \sim 5^{-2/3}$. The values of ν' and η' are 10^{-2} and 2.5×10^{-3}, respectively, and $\delta=1.5$. A seed of magnetic energy of 2% is introduced, and integration proceeds for about 130 turnover times, to $t=45$. Figure 4 shows the time evolution of kinetic and magnetic energies and of magnetic helicity. E^V is decreasing slightly, but E^M and $-H^M$ have an approximately linear growth at long times and show no saturation trend. At $t=45$, $E^M/E^V \approx 2$. At first, magnetic energy builds up near injection wave numbers. Then the peak of the magnetic energy spectrum drifts to smaller wave numbers until it reaches $k_{\min}=1$. It then keeps growing in amplitude at low k. At $t=45$, $E_k{}^M/E_k{}^V \approx 50$ at $k=1$ and the relative magnetic helicity $kH_k{}^M/E_k{}^M$ is -0.96 at $k=2$, i.e., nearly maximal (negative). Hence, the large-scale $\vec{b}$ is mostly force free and produces only very little large-scale motion.

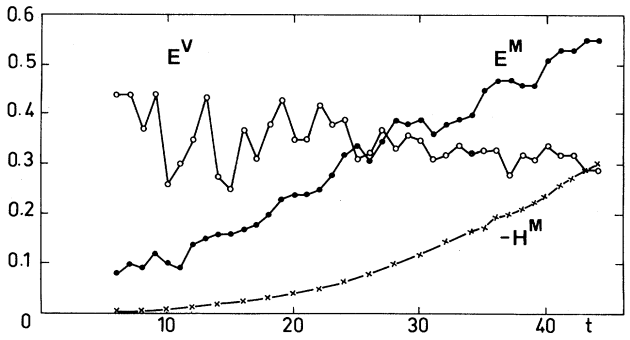

FIG. 4. Helical dynamo with driving at intermediate scales ($k=5$). Temporal variation of kinetic energy (E^V), magnetic energy (E^M), and magnetic helicity ($-H^M$).

The linear growth is consistent with a two-scale model introduced by Kraichnan.[17] The small-scale (here $k\sim5$) dynamics of $\vec{v}$ and $\vec{b}$ in this model includes (i) random helical driving; (ii) coupling between $\vec{v}$ and $\vec{b}$ by Alfvén waves due to a strong large-scale ($k\sim1$) magnetic field $\vec{B}$; (iii) damping by an eddy kinetic and magnetic diffusivity. The α coefficient, defined by $\langle \vec{v}\times\vec{b}\rangle = \alpha\vec{B}$, is then proportional to B^{-2} for large $\vec{B}$.[17] The induction equation for the dynamics of the large-scale $\vec{B}$ becomes, after averaging over the small scales and neglecting Joule dissipation,

$$\partial_t \vec{B} = \nabla\times\langle\vec{v}\times\vec{b}\rangle = \nabla\times\alpha(B)\vec{B}, \qquad (1)$$

with $\alpha(B) = -C\tilde{\epsilon}^V k_0{}^{-2} B^{-2}$. Here, $\tilde{\epsilon}^V$ is the kinetic helicity injection rate, k_0 an injection wave number, and C a positive numerical constant. It should be possible to show that Kraichnan's[17] model and the resulting nonlinear dynamo equation are asymptotically exact for large-scale separation and strong fields. Linear variation of H^M with time is an exact consequence of (1). Indeed, let $\vec{B}=\nabla\times\vec{A}$ and $H^M=(1/2V)\int\vec{B}\cdot\vec{A}\,dV$, where V is the volume of the domain [here $(2\pi)^3$]. A simple calculation then gives $dH^M/dt = C\tilde{\epsilon}^V k_0{}^{-2}$. The monotonic variation of H^M, the drift to small wave numbers of the peak in the magnetic energy (and helicity) spectrum, and the nearly maximal magnetic helicity at $k=1$ are consistent with a previously conjectured inverse cascade of magnetic helicity.[13,18]

We have benefited from discussions with P. A.

Gilman, R. H. Kraichnan, J. Léorat, S. A. Orszag, and G. S. Patterson. We are indebted to the National Center for Atmospheric Research (sponsored by the National Science Foundation) for a generous attribution of computer time. We also wish to thank the entire staff of the National Center for Atmospheric Research Computing Division.

---

[a]On leave from Observatoire de Nice, Nice, France.

[1]H. K. Moffatt, *Magnetic Field Generation in Electrically Conducting Fluids* (Cambridge Univ. Press, Cambridge, 1978); E. N. Parker, *Cosmical Magnetic Field* (Clarendon, Oxford, 1979); F. H. Busse, Annu. Rev. Fluid Mech. 10, 435 (1978).

[2]M. K. Bevir, J. Br. Nucl. Energy Soc. 12, 455 (1973).

[3]J. Léorat, A. Pouquet, and U. Frisch, J. Fluid Mech. 104, 419 (1981).

[4]E. C. Bullard and H. Gellman, Philos. Trans. Roy. Soc. London 12, 455 (1973); A. Herzenberg, and F. J. Lowes, Philos. Trans. Roy. Soc. London, Ser. A 249, 597 (1957); G. E. Backus, Ann. Phys. (N.Y.) 4, 372 (1958); S. I. Braginskii, Zh. Eksp. Teor. Fiz. 47, 2178 (1964) [Sov. Phys. JETP 20, 726 (1964)].

[5]M. Steenbeck, F. Krause, and K. H. Rädler, Z. Naturforsch. 21a, 369 (1966).

[6]A. Pouquet and G. S. Patterson, J. Fluid Mech. 85, 305 (1978).

[7]P. A. Gilman and J. Miller, to be published.

[8]S. A. Orszag and G. S. Patterson, Phys. Rev. Lett. 28, 76 (1972).

[9]R. H. Kraichnan and S. Nagarajan, Phys. Fluids 10, 859 (1967).

[10]Dynamo action will not be suppressed if the diffusion coefficient becomes negative as a consequence of helicity fluctuations. This, however, requires considerable coherence in helicity fluctuations [R. H. Kraichnan, J. Fluid Mech. 75, 657 (1976), and 77, 753 (1976)].

[11]It still has helicity fluctuations on a scale substantially smaller than the integral scale.

[12]These strong fluctuations can be avoided by using a deterministic driving mechanism, e.g., convection, as in Ref. 7.

[13]A. Pouquet, U. Frisch, and J. Léorat, J. Fluid Mech. 77, 321 (1976).

[14]E. D. Siggia, J. Fluid Mech. 107, 375 (1981).

[15]In the closure calculation of Ref. 5, for the same parameters, R_c^M is about 80.

[16]E. A. Speigel, Ann. N. Y. Acad. Sci. 357, 305 (1980).

[17]R. H. Kraichnan, Phys. Rev. Lett. 42, 1677 (1979).

[18]U. Frisch, A. Pouquet, J. Léorat, and A. Mazure, J. Fluid Mech. 68, 769 (1975).